

Accelerated Pavement Testing of Perpetual Pavement Test Sections under Heavy Aircraft Loading at FAA's National Airport Pavement Test Facility

Navneet Garg¹, Qiang Li², and Monir Haggag³

(¹ FAA, William J. Hughes Technical Center, EHT, NJ 08405, USA, Navneet.Garg@faa.gov)

(² CSRA Intl. Inc., 1201 New Road, Linwood, NJ 08221 U.S.A, Qiang.Li@csra.com)

(³ CSRA Intl. Inc., 1201 New Road, Linwood, NJ 08221 U.S.A, Monir.Haggag@csra.com)

ABSTRACT

Six flexible pavements were constructed for construction cycle 7 (CC7), at the Federal Aviation Administration (FAA) National Airport Pavement Test Facility in Atlantic City, New Jersey. Four test sections on the north side include 200 mm (LFP-4), 250 mm (LFP-3), 300 mm (LFP-2), and 375 mm (LFP-1) of hot mix asphalt (HMA) over an aggregate subbase (thickness varying between 850 and 1025 mm) resting on a subgrade with CBR of 6. The fifth test section LFC-5 is conventional flexible pavement with 125 mm of HMA over aggregate base and subbase, and LFC-6 structure is same as LFC-5 except that the crushed stone base layer is replaced with asphalt stabilized drainable base. The objective of CC7 tests is to develop perpetual pavement design criterion, and validate/refine/modify fatigue model for HMA in airport pavement thickness design software FAARFIELD. The HMA fatigue model is based on the ratio of dissipated energy change (RDEC). Four Fiber Optic Strain Plates were installed to measure transverse and vertical strains at top, and transverse stains at bottom within the HMA layer. Full-scale accelerated pavement tests were performed on test sections. Traffic test load parameters were – 6-wheel gear, 245 kN wheel load (gear load 1470 kN), and 4 kmph speed. Pavement performance was monitored using crack maps, straight edge rut depth and surface profile measurements. LFC-5 and LFP-4 showed significant fatigue cracks and rutting. LFP-1 and LFP-2 performed well with no signs of any cracking. This paper presents discussion on RDEC fatigue model, pavement thickness design, pavement materials characterization test results, pavement instrumentation, accelerated pavement tests under heavy aircraft gear loads, and pavement responses measured using embedded sensors. The test section performance shows that under loading conditions used in the study, by increasing HMA thickness from 25.4 cm to 30.5 cm, fatigue cracking was eliminated during the duration of testing (38,000 passes).

Keywords: Accelerated Pavement Tests, HMA, perpetual pavement, fatigue, strains.

1. INTRODUCTION

The Federal Aviation Administration's (FAA) National Airport Pavement Test Facility (NAPTF) is located at the FAA William J. Hughes Technical Center, Atlantic City International Airport, New Jersey. The primary objective of NAPTF is to generate full-scale pavement response and performance data for development and verification of airport pavement design criteria. The test facility consists of a 274 m long by 18.3 m wide test pavement area and a test vehicle for loading the test pavement with up to twelve aircraft tires at wheel loads of up to 334 kN (75,000 lbs). Additional information about the test facility is available elsewhere (<http://www.airporttech.tc.faa.gov>).

1 A construction cycle (CC) at the NAPTF includes test pavement construction including
2 instrumentation, traffic tests to failure, posttraffic testing, and pavement removal. In CC7, six
3 new flexible pavement test sections were constructed on the CBR-6 subgrade. The test sections
4 were designed using FAARFIELD (FAA's airport pavement thickness design software).
5 Pavement instrumentation consisted of H-bar strain gages at the bottom of HMA, an innovative
6 instrumentation Fiber Optic Strain Plate (FOSP) in the four perpetual pavement test sections to
7 measure transverse and vertical strains at top and transverse stains at bottom within the HMA
8 layer, multiple depth deflectometers (MDD's), and pressure cells on top of the subgrade. Traffic
9 tests were performed with six-wheel landing gear with 25 metric ton (55,000 lbs) wheel load
10 (gear load = 150 metric tons). Straight edge rut depth measurements and HMA crack maps were
11 prepared during traffic tests.

12 This paper summarizes the objectives of CC7 tests, new HMA fatigue model
13 incorporated in FAARFIELD, pavement thickness design, and test section performance from the
14 traffic tests.

15 2. OBJECTIVES FOR CC-7 TESTS

16 In the perpetual pavement concept, the pavement failure is limited to the surface layer,
17 and structural failure (rutting in subgrade, bottom-up fatigue cracking) is eliminated. The
18 objectives of this study were to:

- 19 • Develop Perpetual Pavements Design criterion for airport pavements.
- 20 • Determine vertical strain threshold in intermediate HMA layer to limit rutting.
- 21 • Determine horizontal strain threshold in the HMA layer to prevent bottom-up fatigue
22 cracking.
- 23 • Study strain distribution in the HMA layer.
- 24 • Validate/refine the new asphalt fatigue model in FAARFIELD.
- 25 • Determine relationship between laboratory fatigue strain threshold and measured field
26 HMA strains.

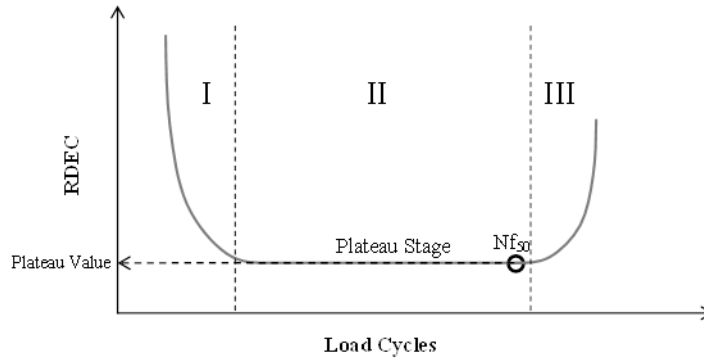
27 3. HMA FATIGUE MODEL IN FAARFIELD

28 FAARFIELD is a computer program for airport pavement thickness design. It
29 implements both layered elastic based and three-dimensional finite element-based design
30 procedures developed by the FAA for new and overlay design of flexible and rigid pavements.
31 The thickness design procedures implemented in the program are the FAA airport pavement
32 thickness design standards referenced in Advisory Circular (AC) 150/5320-6E [1]. Subgrade
33 vertical strain and horizontal strain at the bottom of the HMA layer are the design criteria for
34 flexible pavements. Since the default asphalt modulus value of 1379 MPa (200,000 psi) is fixed,
35 horizontal strain becomes the dominant criterion only for thick pavements subjected to heavy
36 wheel/gear loads. The Heukelom and Klomp model [2] used to determine the number of
37 coverages to HMA fatigue failure for a given horizontal strain at the bottom of the HMA layer is:

$$38 \log_{10}(C) = 2.68 - 5 \times \log_{10}(\epsilon_h) - 2.665 \times \log_{10}(E_A)$$

39 where C is number of coverages to failure, ϵ_h is the horizontal strain at the bottom of HMA layer,
40 and EA is the HMA modulus (in psi). Many studies [3, 4, and 5] have shown that Ratio of
41 Dissipated Energy Change (RDEC) provides a better indication of damage induced by the
42 repeated load. The procedure developed by Carpenter and Shen [6] has been incorporated in the
43 new version of FAARFIELD (currently under review). RDEC is defined as the change of the

1 dissipated energy between two cycles divided by the dissipated energy of previous cycle. There
 2 are three stages in a typical curve of RDEC versus the number of load cycles (Figure 1). A
 3 plateau is established at stage II after the initial period (stage I). The fatigue failure happens at
 4 the stage III where RDEC dramatically increases. The Plateau Value (PV) is the RDEC value
 5 where the stiffness reduces to 50% and has a unique relation with fatigue performance of asphalt
 6 concrete.



9 **FIGURE 1. Typical RDEC versus Load Cycles**

10
 11 In a large number of asphalt beam fatigue tests it has been found that the “plateau value”
 12 (PV) of RDEC is a reliable predictor of the number of cycles to fatigue failure (N_f). For a broad
 13 range of asphalt mixes, this relationship is given by:

$$14 \quad N_f = 0.4801 \times PV^{-0.9007}$$

15 Also, for a given horizontal strain at the bottom of the asphalt layer, the value of RDEC
 16 can be estimated by:

$$17 \quad PV = 44.422 \times \varepsilon_h^{5.14} \times S^{2.993} \times VP^{1.85} \times GP^{-0.4063}$$

18 where PV is the estimated value of the RDEC plateau value (dimensionless), S is HMA flexural
 19 stiffness (psi), ε_h is horizontal strain at the bottom of the asphalt layer, VP is the volumetric
 20 parameter, and GP is gradation parameter. It is important to note that S, the initial flexural
 21 stiffness of an asphalt beam specimen subjected to fatigue cycles, is not the same as the HMA
 22 modulus used to compute strain in the layered elastic analysis. The volumetric parameter VP and
 23 gradation parameter GP are defined as follows:

$$24 \quad VP = V_a / (V_a + V_b) \quad \text{and} \quad GP = (P_{NMS} - P_{PCS}) / P_{200}$$

25 where V_a is air voids, V_b is asphalt content by volume, P_{NMS} is the percent of aggregate passing
 26 the nominal maximum size sieve, P_{PCS} is the percent of aggregate passing the primary control
 27 sieve, and P_{200} is the percent of aggregate passing the #200 (0.075 mm) sieve. For a typical P-
 28 401 HMA mix (P-401 is FAA specification for HMA), the following default values of the above
 29 parameters are assigned in FAARFIELD: $S=600,000$ psi; $V_a=3.5\%$; $V_b=12.0\%$; $P_{NMS}=95\%$;
 30 $P_{PCS}=58\%$; $P_{200}=4.5\%$.

31 **4. PAVEMENT TEST SECTIONS & HMA CHARACTERIZATION**

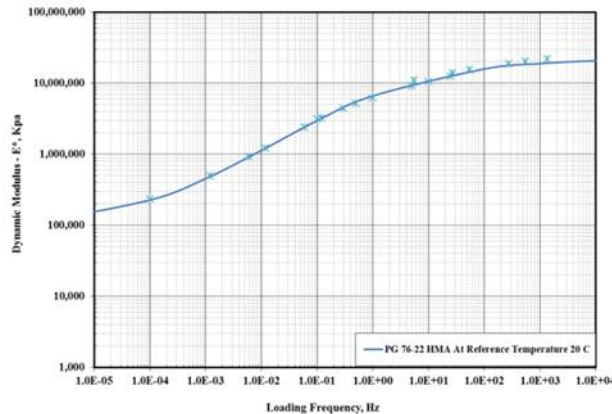
32 For the HMA mix used in CC7, based on mix properties and four-point bending beam
 33 fatigue tests, the following values were assigned in FAARFIELD: $S=871,296$ psi; $V_a=3.4\%$;
 34 $V_b=15.5\%$; $P_{NMS}=95\%$; $P_{PCS}=48\%$; $P_{200}=5.3\%$. The target fatigue lives of the CC7 perpetual

1 pavement test sections varied from 3,636 (for LFP-4N) to 40,000 passes (for LFP-1N). The test
 2 pavements were designed using FAARFIELD and B-777 aircraft with 245 kN (55,000-lbs)
 3 wheel load. The test section thicknesses were designed in such a way so that subgrade failure
 4 occurs in conventional flexible pavement (LFC-5N) and HMA fatigue failure occurs in perpetual
 5 pavement test sections (LFP-1N through LFP-4N). All four of the perpetual pavement test
 6 sections were constructed on a low-strength subgrade, and were labeled as LFP-1N, LFP-2N,
 7 LFP-3N and LFP-4N. Table 1 gives the design thicknesses, and number of passes to HMA
 8 fatigue, and subgrade failure for different test sections, using FAARFIELD.

9 **TABLE 1. Pavement Test Section Design Thicknesses and Passes to Failure**

Test Section	P-401 HMA Thickness, cm	P-209 Base Thickness, cm	P-154 Subbase Thickness, cm	HMA Strain, microstrain	Subgrade Strain, microstrain	Passes to HMA Failure	Coverages to HMA Failure	Passes to Subgrade Failure
LFP-1N	38.0	0	89	524	1298	40,000	61,538	66,667
LFP-2N	30.5	0	94	657	1321	15,385	21,075	40,000
LFP-3N	25.4	0	97	781	1333	7,407	9,376	33,333
LFP-4N	20.3	0	97	932	1345	3,636	4,228	28,571
LFC-5N	12.7	20.3	74	532	1492	50,000	-	4,545

10
 11 The HMA mixture used was FAA P-401 specification [7] material with PG 76-22
 12 polymer modified binder. The aggregate bulk specific gravity was 2.853 and PG76-22 Asphalt
 13 Binder Specific Gravity was 1.03. The optimum asphalt content was 5%. Dynamic modulus was
 14 determined in uniaxial compression using the Universal Testing Machine (UTM-25) following
 15 the method outlined in AASHTO TP-79 “Determining the Dynamic Modulus and Flow Number
 16 for Asphalt Mixtures Using the Asphalt Mixture Performance Tester”. Figure 3 shows the
 17 dynamic modulus master curves for CC7 HMA.



18
 19
 20
 21
 22
 23
 24
 25
 26
 27
 28
 29
 30
 31 **FIGURE 2. CC7 HMA dynamic modulus E* master curve (20 °C ref. temperature)**

32 **5. TRAFFIC TESTS AND TEST SECTION PERFORMANCE**

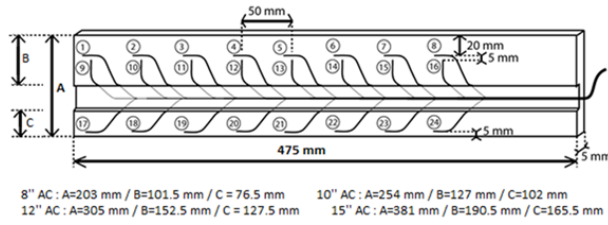
33 The CC-7 north lane was trafficked by a six-wheel triple dual tandem (3D) gear
 34 configuration at 1372 mm (54 in) dual spacing and 1449 mm (57 in) tandem spacing. Wheel
 35 loads were set at 245 kN (55,000 lbs) each. This gives “strut” loads of 1468 kN (330,000 lbs).
 36 The traffic speed was 4 km/h (2.5 mph).

1 A fixed wander pattern was applied to the traffic during the tests. The wander pattern
2 consisted of 66 repetitions, 33 traveling east and 33 traveling west. The transverse position of the
3 gears was changed only at the start of the eastward repetitions. The wander pattern was designed
4 to simulate a normal distribution with standard deviation of 775 mm (30.5 in) (equivalent to a
5 taxiway distribution for design). The distribution of the transverse wheel positions is not random,
6 but consists of nine equally spaced wheel paths at intervals of 260 mm (10.25 in). The failure
7 criteria used for flexible pavements are: 1) 25.4-mm (1-in) upheaval outside the traffic lane,
8 signifying structural shear failure in the subgrade or other supporting layers; and 2) surface
9 cracking to the point that the pavement is no longer waterproof, signifying complete structural
10 failure of the surface layer. These are the same criteria as used for the multiple wheel heavy gear
11 load (MWHGL) test series run by the U.S. Army Corps of Engineers Waterways Experiment
12 Station in early 1970's.

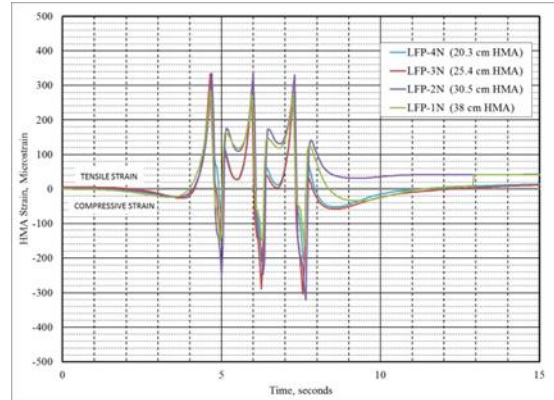
13 Pavement performance during traffic tests was monitored using Fiber Optic Strain Plates
14 (to monitor HMA strains), Straight Edge Rut Depth (to monitor rutting), and Crack Maps. Most
15 of the traffic tests on north side test sections were performed during winter months. Pavement
16 temperatures (measured at mid-depth of LFP-1N at 19 cm) were as follows: Maximum = 25.6°C
17 (78°F), Minimum = -1.1°C (30°F), Mean = 10°C (50°F), standard deviation = 8.4, and
18 Coefficient of variation (COV) was 16.8 percent. After completion of 23,364 passes test sections
19 LFC-5N and LFS-6N were declared failed due to the presence of severe alligator or fatigue
20 cracking, and traffic tests were terminated for these two test sections. Traffic tests were
21 continued on the perpetual pavement test sections (LFP-1N through LFP-4N). Traffic tests were
22 terminated on LFP-4N after completion of 27,192 passes, and LFP-3N after completion of
23 35,046 passes due to the presence of severe fatigue cracking. After completion of 30,030 passes,
24 traffic tests were continued on LFP-1N, LFP-2N, and LFP-3N at increased wheel load of 289 kN
25 (65,000 lbs). Traffic tests were terminated on these two sections after completion of 37,686
26 passes with no evidence of any fatigue cracks. The following sections will present strains
27 measured in HMA layer using FOSP, straight edge rut depth measurements, and crack maps.

28 Four "strain plates" supporting an array of 24 Fabry-Perrot fiber optic sensors were
29 retrofitted in the HMA layers of four perpetual pavement test sections (LFP-1N, LFP-2N, LFP-
30 3N). The strain plates allow for the measurement of near -surface compressive and tensile strains
31 as well as tensile strains at the bottom of the AC layer over an 18 inch (45 cm) width across the
32 wheel path. Data obtained from the strain plates under a moving wheel can be used to produce
33 detailed strain basins across the entire tire width, allowing for a detailed analysis of the effect of
34 tire type, load and pressure on pavement response. The HWD deflection measurements showed
35 that the installation of strain plates does not alter the pavement structure significantly and forms
36 an integral part of the pavement structure. More detailed information can be found in reference
37 [8]. Figure 3 (a) shows the schematic of the FOSP and 3(b) shows the vertical strains measured
38 close to the HMA surface. The vertical strains are measured 25 mm below the HMA surface. As
39 the wheel approaches sensors, the strains are slightly compressive in nature, and then become
40 tensile resulting in first peak, strains start reducing significantly and become compressive in
41 nature as the second axle approaches, and same follows with the third axle. The magnitude of
42 maximum tensile strains is similar to the magnitude of maximum compressive strains (observed
43 between the axles). Similar strain magnitudes are observed in all four test sections. Figure 4
44 shows transverse strains measured at the bottom and top of the HMA layer. Three peaks are
45 observed due the presence of three axles in the gear configuration. The strains are tensile in
46 nature and occur when wheels are directly above the sensors. As the wheel approaches sensors,

1 the tensile strains increase resulting in first peak, strains start reducing and increase again as the
 2 second axle approaches, and same follows with the third axle.
 3

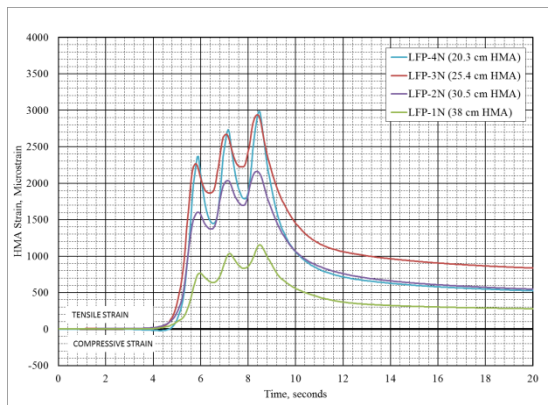


(a) Transverse strains at bottom of HMA layer

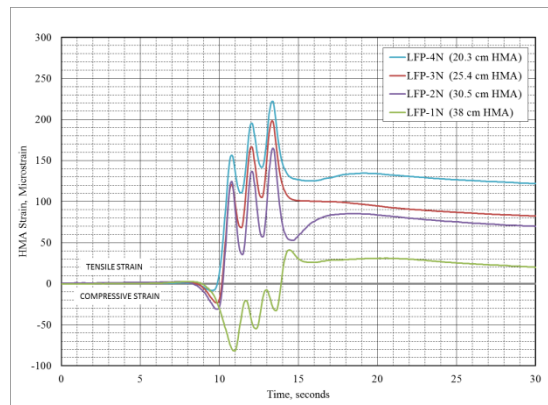


(b) Vertical strains close to HMA surface

4 **FIGURE 3. FOSP layout and Vertical Strains in HMA**
 5



(a) Transverse strains at bottom of HMA layer



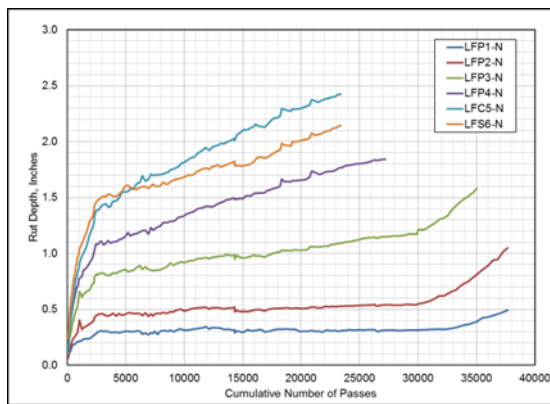
(b) Transverse strains at HMA surface

6 **FIGURE 4. Transverse strains measured in HMA layer**
 7

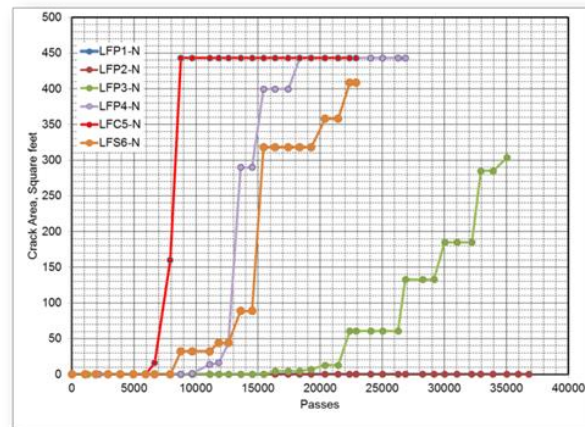
8 Another important feature of strain-time history curve shown in Figure 4 is the
 9 accumulation of permanent strain in transverse direction. As the first axle passes over the strain
 10 plate, the strain is not completely recovered and the second axle passes over it, followed by the
 11 third axle. This results in un-symmetrical strain response curve and permanent strain
 12 accumulation. This accumulation of transverse strain results in the longitudinal crack (first
 13 cracks observed in the pavement). The magnitude of maximum tensile strains is also affected by
 14 the HMA thickness with lower peak strains for thicker HMA layer. Severe fatigue cracks were
 15 observed in LFP-3N and LFP-4N. The numerous cores extracted showed evidence of top-down
 16 cracking. No evidence of bottom-up cracking was found. Figure 4 (b) shows maximum strains
 17 observed at close to surface of HMA layer. The maximum tensile strains occur when the sensors
 18 are adjacent to the gear (outside, with all wheels away from sensor). As the wheel approaches
 19 sensors, the strains are compressive in nature and then increase resulting in first peak, strains
 20 start reducing and increase again as the second axle approaches, and same follows with the third

1 axle. HMA thickness affects the position of gear with respect to the sensor for maximum tensile
 2 strains. The magnitude of maximum tensile strains at the HMA surface is also affected by the
 3 HMA thickness with lower peak strains for thicker HMA layer.

4 A 5-meter (16-foot) long aluminium straight edge was used for measuring surface ruts.
 5 Figure 5(a) shows the rut depth measurements for all the six flexible pavement test sections.
 6 Figure shows that the conventional flexible pavement LFC-5N exhibited maximum rutting, and
 7 performed worse than the test section with asphalt drainable base (LFS-6N). Among the
 8 perpetual pavement test sections, pavements with thicker HMA surface performed better. There
 9 was no significant change in surface rutting observed in LFP-1N and LFP-2N from 5,000 passes
 10 to 30,030 passes till the increase in wheel load from 245 kN to 289 kN. Analysis of MDD data
 11 showed that for perpetual pavement test sections LFP-1N and LFP-2N, most of the rutting was
 12 contributed by the subbase layer. For test sections LFP-3N and LFP-4N, most of the rutting was
 13 contributed by subbase and subgrade. After completion of CC-7 traffic tests, transverse trenches
 14 will be cut to study the failure mechanism, and quantify the contribution of each layer to total
 15 surface rutting. Figure 5(b) shows the progression of surface cracks with number of passes.



(a) Straight edge rut depth measurements
 (1 inch = 2.54 cm)



(b) Progression of fatigue cracks during traffic tests
 (1 sq.foot = 0.093 sq.m)

FIGURE 5. Pavement Performance

19 Significant fatigue cracks (alligator cracks) were observed in LFC-5N at 6,666 passes,
 20 LFP-4N at 11,814 passes (13,737 coverages), and LFP-3N at 21,450 passes (27,152 coverages).
 21 Test sections LFP-1N and LFP-2N showed no evidence of fatigue cracking. When comparing the
 22 predicted number of passes to failure (see Table 1) with observed number of coverages to failure,
 23 for conventional flexible pavement LFC-5N, the pavement showed significant fatigue cracking at
 24 7,000 passes compared to 50,000 as predicted by the model. Significant rutting in pavement
 25 structure accentuated the fatigue cracking causing section to fail much earlier. For test section
 26 LFP-4N, the observed number of coverages to failure (13,737) is about 3.25 times the predicted
 27 number of coverages (4,228), and for LFP-3N the observed number of coverages to failure
 28 (27,152) is about 2.9 times the predicted number of coverages (9,376). Fatigue failure in
 29 laboratory beam fatigue test is defined as when the stiffness of beam is half of the initial
 30 stiffness. In APT, the fatigue failure is the presence of significant alligator cracks in the test
 31 pavement, and hence the factor of about three between predicted and observed fatigue life.

1 **6. SUMMARY**

2 Full-scale traffic test results from FAA’s NAPTF construction cycle 7 flexible pavements
3 have been presented. The objective of CC7 tests is to develop perpetual pavement design
4 criterion, and validate/refine and/or modify the newly incorporated fatigue model for hot mix
5 asphalt (HMA) in airport pavement thickness design software FAARFIELD. Two of the thicker
6 perpetual pavement test sections (LFP-1N and LFP-2N) did not show any evidence of fatigue
7 cracks, whereas LFP-3N and LFP-4N showed severe fatigue cracking. All the cracks were found
8 to be top-down cracks. The conventional flexible pavement test section LFC-5N showed severe
9 rutting and fatigue cracking. The test section performance shows that under given aircraft gear
10 loading used in the study, by increasing HMA thickness from 25.4 cm to 30.5 cm, fatigue
11 cracking was eliminated during the duration of testing (almost 38,000 passes). FOSP strain
12 measurements were useful in understanding the HMA layer behavior. Laboratory fatigue tests
13 were performed to determine input properties for the fatigue model incorporated in FAARFIELD
14 and comparison was made between predicted and observed fatigue life. The comparison showed
15 that the observed fatigue life of test sections (that exhibited fatigue cracking) is about 2.9 to 3.25
16 times the predicted fatigue life. This would suggest that it would take significantly large number
17 of passes to initiate fatigue cracks in LFP1 and LFP2. For validating and refining the fatigue
18 model implemented in FAARFIELD, more data is needed. More flexible pavement tests are
19 planned as part of CC9.
20

21 **7. REFERENCES**

22 [1] Federal Aviation Administration Office of Airport Safety and Standards, “Airport Pavement
23 Design and Evaluation”, Advisory Circular AC 150/5320-6E, U.S. Department of Transportation,
24 2009.
25 [2] Heukelom, W. and A. J. G. Klomp, “Dynamic Testing as a Means of Controlling Pavements
26 During and After Construction.” Proceedings International Conference on the Structural Design
27 of Asphalt Pavements, Ann Arbor, Michigan, United States, 1962.
28 [3] Ghuzlan, K., “Fatigue Damage Analysis in Asphalt Concrete Mixtures Based Upon
29 Dissipated Energy Concepts,” Ph.D. Thesis, University of Illinois at Urbana-Champaign, Urbana,
30 IL, 2001.
31 [4] Carpenter, S. H., and Jansen, M., “Fatigue Behavior under New Aircraft Loading
32 Conditions.” Proceedings of Aircraft Pavement Technology in the Midst of Change, Seattle,
33 Washington, United States, 1997.
34 [5] Ghuzlan, K, and Carpenter, S. H., “Energy-Derived/Damage-Based Failure Criteria for
35 Fatigue Testing,” Transportation Research Record: Journal of the Transportation Research Board,
36 Vol. 1723, pp. 141-149, 2000.
37 [6] Shen, S., and Carpenter, S. H., “Development of an Asphalt Fatigue Model Based on Energy
38 Principles”, Journal of the Association of Asphalt Paving Technologists, Vol. 76, Association of
39 Asphalt Paving Technologists, 2007.
40 [7] FAA, AAS-100, Office of Airport Safety & Standards, 150/5370-10G - Standards for
41 Specifying Construction of Airports, U.S. Department of Transportation, 2014.
42 [8] Garg, N., Bilodeau, J-P, Dore, G., “Experimental Study of Asphalt Concrete Strain
43 Distribution in Flexible Pavements at the National Airport Pavement Test Facility”, FAA
44 Technology Transfer Conference, Atlantic City, NJ, 2014.